

UV-A photochemistry of the pesticide azinphos-methyl: Generation of the highly fluorescent intermediate N-methylantranilic acid

Lovely Yeasmin, Shawn A. MacDougall, Brian D. Wagner*

Department of Chemistry, University of Prince Edward Island, 550 University Ave, Charlottetown, P.E.I., Canada C1A 4P3

ARTICLE INFO

Article history:

Received 19 December 2008
Received in revised form 11 March 2009
Accepted 26 March 2009
Available online 5 April 2009

Keywords:

UV photolysis
Azinphos-methyl
Organophosphate pesticides
Fluorescence
Pesticide photochemistry
N-Methylantranilic acid

ABSTRACT

Azinphos-methyl (AZM) is a widely used organophosphate insecticide and acaricide, with demonstrated negative impacts on the environment. Upon absorption of UV-A radiation, this molecule undergoes photolysis to the highly fluorescent compound N-methylantranilic acid, which undergoes subsequent photolysis to photochemically stable products. The identity of N-methylantranilic acid as the highly fluorescent photochemical intermediate was determined by fluorescence spectroscopy, and the identity of benzazimide as the major final photoproduct was determined by ¹H NMR spectroscopy and high performance liquid chromatography. A detailed UV-A photolysis mechanism is proposed, involving two pathways, the major one leading to benzazimide as the stable photoproduct, and the other to N-methylantranilic acid as an intermediate and aniline as a final stable photoproduct. This photolysis has implications for fluorescence-based trace analysis of this pesticide, as controlled UV exposure results in significant fluorescence enhancement of AZM in solution via formation of the highly fluorescent intermediate N-methylantranilic acid. It also has importance in the environmental fate of this pesticide, as the UV-A in sunlight is found to decompose an aqueous solution of this pesticide over the course of a single day.

© 2009 Elsevier B.V. All rights reserved.

1. Introduction

Azinphos-methyl (AZM), shown in Fig. 1, is a highly efficient organophosphate insecticide and acaricide [1,2]. It has found significant agricultural use in Canada as well as other parts of the world. AZM is relatively persistent, and has a high toxicity to non-target species, including fish and other aquatic species which are exposed via field run-off or spray drift [3]. It has a relatively high water solubility of 29 ppm [2]. This pesticide is thus of significant environmental concern, as a result of this potential for negative impact on natural waters [3,4]. For example, in the past 10 years regular fish-kill incidents have occurred in streams in the Canadian province of Prince Edward Island; these have been related to the effects of agricultural run-off water containing high levels of pesticides, including AZM. High levels of AZM, as well as other pesticides, have also been recently measured in the atmosphere in specific agricultural regions across Canada [5].

Previous work in our laboratory showed that the weak natural fluorescence of AZM in aqueous solution can be enhanced in a variety of ways, including UV photolysis, inclusion into cyclodextrins, and base hydrolysis [6]. In this work, we have focused on the UV photolysis of AZM, to determine the identity of the highly

fluorescent species generated photochemically from AZM, and to elucidate the mechanism of its photochemical formation. By using UV-A radiation, at a wavelength of 350 nm, these results can be used to model the effect of sunlight on AZM in natural waters, and thus have important implications on the environmental fate of this potentially harmful pesticide.

There have been a number of previous studies of the photochemistry of this important pesticide [7–11]. The first two [7,8] were reported nearly 40 years ago, and described photolysis products only, as determined by thin layer chromatography, with no identification of intermediates or proposal of a photochemical mechanism. In both cases, a number of major photolysis products were identified, mostly benzazimide (BA) derivatives, as well as a small amount of anthranilic acid (AA). The latter is a likely candidate for the highly fluorescent species observed in our previous work [6], as this is also the fluorescent product which results from base hydrolysis of azinphos-methyl [12,13]. In fact, base-catalyzed conversion to anthranilic acid has been used in fluorescence-based trace analysis of azinphos-methyl [6,12,13]. There were no subsequent photochemical studies of AZM reported until the past 2 years, when three new studies were published [9–11]. The most important, complete, and detailed study is that of Sarakha and co-workers published in this journal in 2007 [9]. They used excitation wavelengths in the range of 254–313 nm, and found that the photolysis quantum yield decreased with increasing excitation wavelength. They determined that several products were formed in

* Corresponding author. Tel.: +1 902 628 4351; fax: +1 902 566 0632.
E-mail address: bwagner@upe.ca (B.D. Wagner).

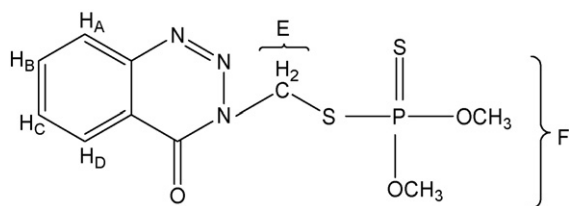


Fig. 1. The chemical structure of azinphos-methyl, with protons labeled for ^1H NMR identification.

aqueous solution, with 1,2,3-benzotriazin-4-(3H)-one, *i.e.* benzazimidate (BA), being the major primary photoproduct, but that it in turn was photolyzed to anthranilic acid. A complete photochemical mechanism was proposed, involving an iminoketene intermediate. Also in 2007, Trebše and co-workers reported the photochemistry of four organophosphate pesticides in aqueous solution, including AZM, using UV-B light, and analyzed the intermediates and products via gas chromatography–mass spectroscopy, and also studied the kinetics of the photochemical reactions [10]. They also observed a number of products, including two triazines as well as anthranilic acid. Finally, in 2008, Calza et al. used titanium dioxide to catalyze complete photochemical degradation of three organophosphorous pesticides, including AZM, using a lamp designed to simulate the solar light [11]. They identified aniline as the ultimate, stable photoproduct of AZM photolysis.

In addition to these photolysis studies of AZM, there has also been a recent, detailed report of the photolysis of the related pesticide azinphos-ethyl (AZE) in cyclohexane and methanol [14]. In this case, a broader range of photoproducts were isolated and identified, and a detailed mechanism was proposed. Of particular interest is the identification of *N*-methylantranilic acid (NMA) as a photoproduct, as opposed to the anthranilic acid reported in the AZM photolysis studies [7–10].

It is important to note that the fluorescence of the photochemical intermediates and products was not reported in any of these previous studies of the photochemistry of AZM, nor in that of AZE. This is the principal aim of this paper, as not only does fluorescence provide a unique and informative method for studying both the kinetics and mechanism of AZM photolysis, but it also has practical applications in the UV-enhanced fluorescence-based trace detection of AZM in water samples. Furthermore, we show that in both water and methanol, *N*-methylantranilic acid is formed from the initial UV-A photolysis of AZM, not anthranilic acid as previously reported [7–10], and furthermore that it is an intermediate, and itself undergoes photochemical reaction, resulting in the formation of aniline as an ultimate, photostable product. Furthermore, we are using UV-A irradiation instead of UV-B as used in most previous studies, in order to model the UV component of solar radiation at the earth's surface, and also report on the photolysis of AZM in direct sunlight, and discuss the implication on its environmental fate and residence time.

2. Experimental

2.1. Materials

The following compounds were obtained from the indicated sources and used as received: azinphos-methyl (AZM), anthranilic acid (AA), *N*-methylantranilic acid (NMA) and benzazimidate (BA) were all received from Sigma–Aldrich; methanol- d_4 was received from CDN Isotopes. Water used was either deionized prepared in lab using distilled water and an Ultrapure ion exchange system, or natural water collected from a Prince Edward Island stream in early spring (before any seasonal agricultural pesticide use).

2.2. Solution preparation

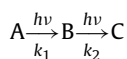
Three types of solutions of azinphos-methyl pesticide were prepared using distilled deionized water, methanol, and methanol- d_4 for the photolysis of AZM in the photoreactor. The concentration of the pesticide in each solvent was 4.0×10^{-5} M; this gave an appropriate absorbance for the fluorescence studies. The solutions were prepared by dissolving 0.0012 g of AZM into 100.0 mL of each solvent. In methanol, AZM was found to be readily dissolved, whereas aqueous solutions required 1 h of sonication, because the concentration of 12 ppm used for the photolysis experiments is close to the aqueous solubility limit of AZM of 29 ppm. All of the solutions were kept sealed in a dark cupboard in the laboratory at room temperature.

2.3. Fluorescence spectroscopy

All absorption and fluorescence measurements were performed on solutions in 1 cm² quartz cuvettes at 22 ± 1 °C. Absorption spectra were measured on a Cary 50 Bio UV–vis Spectrophotometer. Fluorescence spectra were measured on a Photon Technologies International LS-100 luminescence spectrometer, with excitation and emission monochromator bandpasses set at 3 nm and an excitation wavelength of 315 nm. Fluorescence quantum yields were determined using a secondary (relative) method, with 9,10-diphenyl-anthracene as the fluorescent standard ($\phi_F = 0.90$) [15].

2.4. Photolysis and kinetic studies

All photochemical experiments were performed at room temperature using a photoreactor, equipped with a set of 16 UV-A fluorescent tubes (maximum emission at 350 nm) arranged in a circular pattern. A special in-house constructed holder was used to reproducibly place the fluorescence cuvette containing the AZM solution in the centre of the reactor. After a given exposure time (determined cumulatively), the cuvette was removed from the photoreactor, the fluorescence spectrum was measured, and the intensity (I) at 410 nm was recorded. Kinetic plots of I/I_0 versus total irradiation time (t_{irr}) were constructed from the fluorescence data, where I_0 is the fluorescence intensity before irradiation. Based on the observed shape of this plot, which consisted of an initial growth of the fluorescence signal followed by a subsequent decay, it was assumed that there is only one intermediate that fluoresces significantly. This provides a very simple kinetic analysis of the fluorescence data, based on the following three-species model for the growth then decay of the highly fluorescent intermediate B (with A and C as the precursor and final product, respectively):



This is a well-known kinetic model (consecutive first order reactions), for which the following well-known equation can be derived:

$$\frac{I(t)}{I_0} = A \times \frac{k_1}{(k_2 - k_1)(e^{-k_1 t} - e^{-k_2 t})} \quad (1)$$

where A = pre-exponential factor; k_1 = rate constant of the reaction $A \rightarrow B$; and k_2 = rate constant of the reaction $B \rightarrow C$. Kinetic fits were performed using the non-linear curve fitting capability of the commercial Fig-P software program, based on Eq. (1).

2.5. NMR spectroscopy

^1H NMR spectra of methanol- d_4 solutions were obtained on a Bruker Avance 300 MHz ultra-shield instrument with tetramethylsilane (TMS) as an internal standard. Solutions were made with concentrations of 1.5×10^{-3} M for AZM, and 3.6×10^{-3} M for

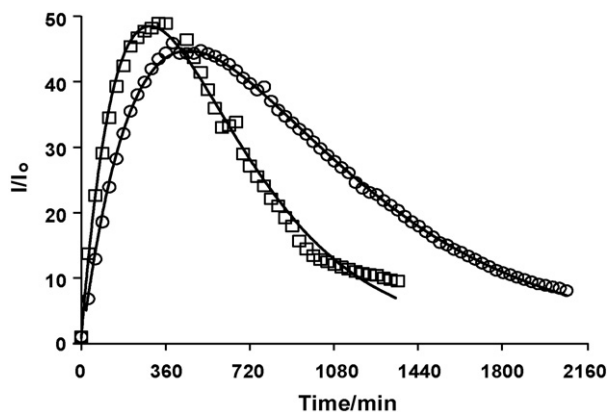


Fig. 2. The fluorescence of 4.0×10^{-5} M solutions of AZM in water (○) and in methanol (□) as a function of exposure time in the 350 nm photoreactor. The solid lines shows the fit to Eq. (1), yielding $k_1 = 0.0023 \text{ min}^{-1}$ and $k_2 = 0.0031 \text{ min}^{-1}$ for water and $k_1 = 0.0036 \text{ min}^{-1}$ and $k_2 = 0.0033 \text{ min}^{-1}$ for methanol.

N-methylantranilic acid, anthranilic acid, and benzazimide. For irradiated solutions, samples were placed in the photoreactor as described above; after the desired irradiation time, the cuvette was removed from the photoreactor, and transferred to an NMR tube.

2.6. HPLC measurements

HPLC analysis was performed with a Varian 400 auto sampler system. All solutions were made at a concentration of 2.5×10^{-4} M. The AZM solutions for photolysis were placed in the photoreactor as described above; after the desired irradiation time, the cuvette was removed from the photoreactor, and a $20 \mu\text{L}$ of the sample was injected for each analysis. The column used was a Pursuit™ C₁₈ reversed-phase column, and the solvent was 60/40 water–methanol (v/v). A UV/vis dual wavelength detector at 285 nm was used, and the pump was a Prostar 210. Optimal separation of the peaks was achieved with 20 min run time. In order to compare retention time of the photoproducts with the standards, the instrument, the column and the detection wavelength were the same as for the qualitative analysis.

3. Results and discussion

3.1. Fluorescence-based studies of the kinetics and mechanism of the UV-A photolysis of AZM

Fluorescence spectroscopy provides a unique and informative experimental method to measure the kinetics of the mechanism for the UV-A photolysis of AZM, as well as the identification of intermediates and products. This is done very simply, by measuring the fluorescence emission of an AZM sample after various exposure times in a UV-A photoreactor. Fig. 2 shows the results for AZM in water and in methanol. In both solvents, a more highly fluorescent intermediate is initially formed, resulting in a large initial increase in fluorescence intensity. However, the intensity is seen to reach a maximum value after 8 h in water (slightly faster at around 6 h in methanol), then the signal decreases, as the intermediate itself is photolyzed to much less fluorescent species. Thus, in both solvents, the model proposed in Scheme 1 holds true, and the data were able to be well fit to Eq. (1), to obtain rate constants for the growth of the highly fluorescent intermediate (k_1) and its decay to less fluorescent photoproducts (k_2). This kinetic model was also found to be valid in deuterated methanol; the kinetic fit results to Eq. (1) are shown in Table 1 for all three solvents.

As can be seen in Table 1, there is a strong solvent dependence, which differs for k_1 and k_2 . The rate of formation of the highly flu-

Table 1

Rate constants for the step-wise photolysis of AZM at 350 nm (average of two trials).

Solvent	k_1/min^{-1}	k_2/min^{-1}
Water	0.0023 ± 0.0001	0.0023 ± 0.0011
Methanol	0.0040 ± 0.0006	0.0038 ± 0.0008
Methanol-d ₄	0.0041 ± 0.0007	0.0017 ± 0.0001

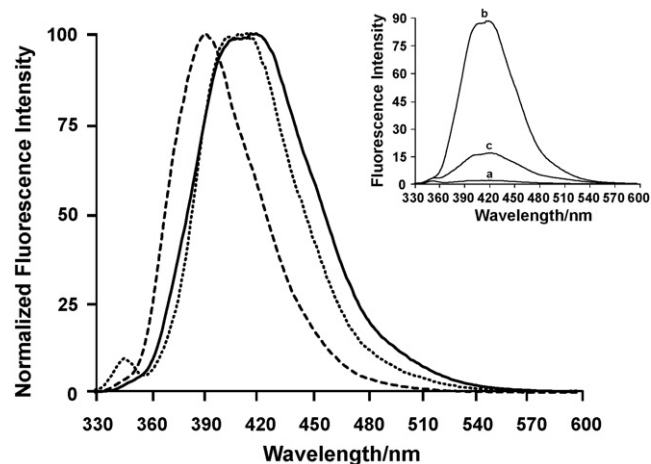


Fig. 3. The normalized fluorescence spectrum of a 4.0×10^{-5} M solution of AZM in water after 8 h exposure (—), as well as those of anthranilic acid (---) and N-methylantranilic acid (...). The inset shows the fluorescence of the AZM in water solution before photolysis (a), after 8 h exposure (b), and after 15 h exposure (c).

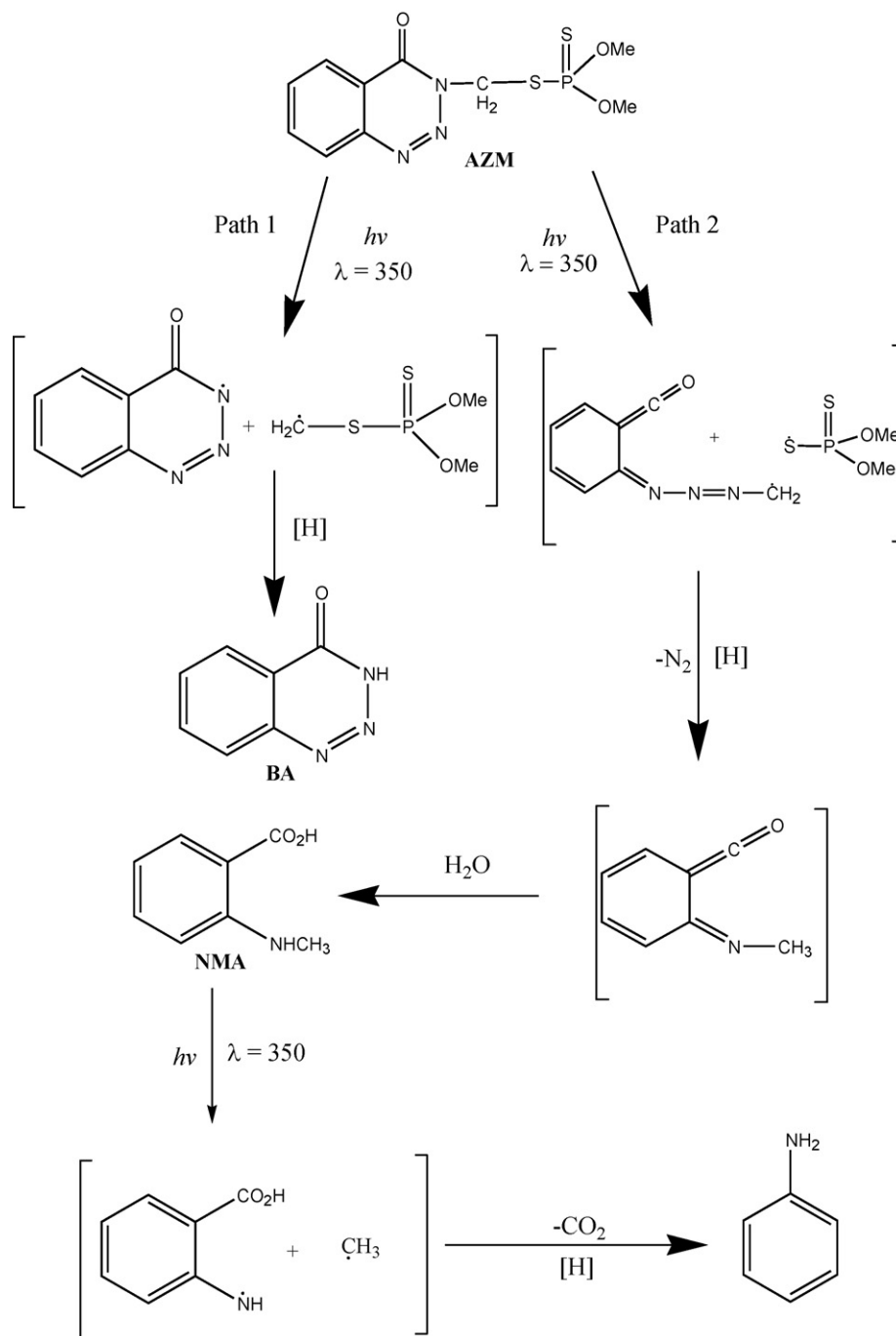
orescent intermediate, as indicated by k_1 , increases in methanol as compared to water; this may be an effect of solvent polarity, indicating a less polar transition state as compared with the starting material, or may involve specific reaction with solvent. However, this formation of the intermediate does not involve hydrogen atom transfer from the solvent, as there is no deuterium isotope effect; the rate constant is identical in methanol and deuterated methanol. In the case of the rate constant for the decay of the intermediate, k_2 , a similar increase in rate is observed in methanol as compared to water. However, in this case there is a strong deuterium isotope effect of $k_{\text{H}}/k_{\text{D}} = 2.2$ in methanol, indicating that direct hydrogen atom transfer from solvent is occurring in this step. Thus, the overall photolysis seems to be leading towards less polar compounds, with H-abstraction from solvent occurring in the decay of the highly fluorescent intermediate.

Fig. 3 shows the effect of UV-A irradiation on the fluorescence spectrum of AZM in water. The inset shows the spectrum of the aqueous AZM solution as a function of UV-A irradiation time, clearly showing the difference in the intensity of the fluorescence emission of AZM, the intermediate, and the final product. In order to identify the intermediate, fluorescence spectra of likely candidates, including anthranilic acid, N-methylantranilic acid, and benzazimide were measured for comparison. The emission maxima of all of these compounds, as well as that of AZM and the photolysis intermediate (after 8 h UV-A exposure), are tabulated in Table 2, which shows an excellent agreement in the wavelength maximum of the pho-

Table 2

Fluorescence emission maxima for various compounds of interest in water and methanol.

Compound	$\lambda_{\text{F,max}}/\text{nm}$ water	$\lambda_{\text{F,max}}/\text{nm}$ methanol
Azinhpos-methyl	419	417
Anthranilic acid	390	395
N-methylantranilic acid	407	405
Benzazimide	400	410
Fluorescent intermediate	407	405



Scheme 1.

tolysis intermediate and N-methylantranilic acid. This is shown graphically in Fig. 3, which shows the normalized spectrum of the intermediate as well as anthranilic acid and N-methylantranilic acid. The spectrum of the intermediate matches very well with that of N-methylantranilic acid, but is significantly red-shifted from that of anthranilic acid. The only significant difference is a broadening of the intermediate emission spectrum relative to that of N-methylantranilic acid, which is postulated to be a result of the much lower absolute intensity of the intermediate spectrum due to its lower generated concentration, which necessitated a significant scaling factor when normalized to match the peak intensity of the N-methylantranilic acid solution. Thus, it is clear from Fig. 3 and Table 2 that the highly fluorescent intermediate is N-methylantranilic acid (at least under UV-A irradiation conditions),

and not anthranilic acid itself, as previously reported [7–10], but in agreement with the previous report on the photolysis of azinphos-ethyl [14]. The same conclusion can be reached for the photolysis of AZM in methanol, as shown in Fig. 4: Table 2 and this figure clearly show that the highly fluorescent intermediate in this solvent is also N-methylantranilic acid, with an even clearer agreement between the spectrum of the highly fluorescent intermediate and that of N-methylantranilic acid shown in Fig. 4 than was observed in water.

To provide further support for the assignment of the highly fluorescent intermediate as N-methylantranilic acid, and to verify its UV-A photolysis, a solution of NMA in methanol was photolyzed in the photoreactor, and its fluorescence measured as a function of exposure time. The resulting data was found to fit very

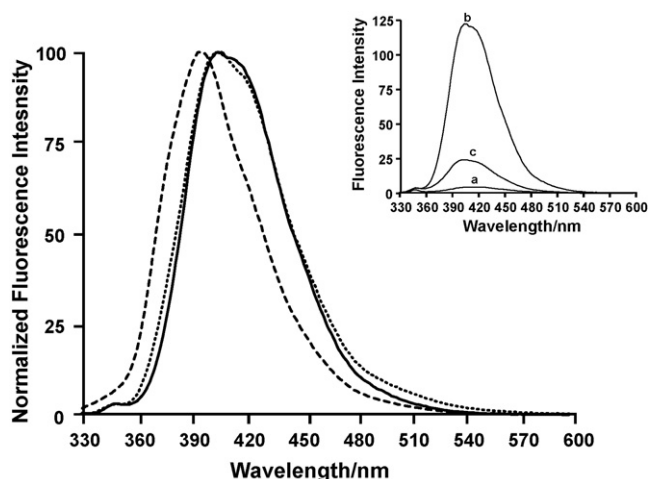


Fig. 4. The normalized fluorescence spectrum of a 4.0×10^{-5} M solution of AZM in methanol after 6 h exposure (—), as well as those of anthranilic acid (---) and N-methylantranilic acid (...). The inset shows the fluorescence of the AZM in methanol solution before photolysis (a), after 6 h exposure (b), and after 15 h exposure (c).

well to a simple first-order exponential decay curve (as shown by the solid line; $r=0.994$), giving a rate constant for its decay of $0.0041 \pm 0.0005 \text{ min}^{-1}$. This is in excellent agreement with the first order rate constant of $0.0038 \pm 0.0008 \text{ min}^{-1}$ measured in the AZM experiment for the decay of the highly fluorescent intermediate. By contrast, photolysis of anthranilic acid also showed first order decay kinetics, but with a significantly higher rate constant of $0.0050 \pm 0.0005 \text{ min}^{-1}$.

An estimate of the peak concentration of N-methylantranilic acid in the photolysis solution can be obtained from the observed peak enhancement of the initial AZM solution (at 8 h irradiation), and the fluorescence quantum yields and extinction coefficients of NMA and AZM. The peak enhancement was found to be a factor of 46.0, and the fluorescence quantum yields of NMA and AZM were determined to be 0.25 ± 0.01 and $7.0 \pm 0.9 \times 10^{-4}$, respectively, allowing an estimate of the peak NMA concentration of 1.6×10^{-5} M in the solution after 8 h irradiation. Thus, NMA conversion from AZM only reaches a maximum of 4% (by mole). The large enhancement observed is a result of the fact that NMA is very much more fluorescent than AZM, with a fluorescence quantum yield a factor of 360 larger.

This observation of the subsequent photolysis of the photogenerated highly fluorescent N-methylantranilic acid has implications for the use of UV photolysis for enhancing the fluorescence-based trace analysis of AZM previously proposed by our group [6]. There would need to be critical testing of any such protocol to establish the optimal UV exposure time for a given photoreactor or other UV lamp set-up for maximum fluorescence enhancement, as over-exposure will reduce the enhanced fluorescence signal. In addition, there is a significant possibility for interference from fluorescence emission from other species in natural water samples. However, this method has potential as a method for trace analysis of AZM, due to the relative ease and lower expense of fluorescence versus HPLC measurements.

3.2. Photolysis of AZM studied by ^1H NMR spectroscopy and HPLC

In order to further explore the identity of the intermediate and products obtained upon UV-A photolysis of AZM, ^1H NMR spectroscopy was performed on unphotolyzed and photolyzed AZM solution in methanol- d_4 , as well as N-methylantranilic acid, anthranilic acid, and benzazimide for comparison. It should be

noted that ^1H NMR spectroscopy was not used in any of the previous studies of the photochemistry of AZM [7–11]. The ^1H NMR spectrum of AZM showed peaks at 8.35, 8.24, 8.11 and 7.98 ppm for the four aromatic protons of AZM (labeled A to D in Fig. 1), and peaks at 5.81 and 3.76 ppm correspond to the non-aromatic protons (labeled E and F, respectively in Fig. 1).

After 6 h of exposure of this solution in the photoreactor (to provide maximum concentration of the intermediate, based on the kinetic results shown in Fig. 2), only one new, very weak peak could be observed in the ^1H NMR spectrum. This peak did not match with any peak found for the spectrum of potential intermediate and products, namely anthranilic acid, N-methyl anthranilic acid, and benzazimide, and remains unidentified.

After 36 h irradiation (to complete the photolysis and obtain final products, the ^1H NMR spectrum of the photolysis mixture showed that all peaks for the AZM band in the aromatic region disappeared, and new peaks had appeared at 8.32, 8.19, 8.09, 7.92, 5.80 and 3.79 ppm. The first four peaks match very well to the spectrum of benzazimide, which showed aromatic proton peaks at 8.32, 8.19, 8.09 and 7.92 ppm. The remaining two peaks at 5.80 and 3.79 ppm could be from other unidentified final product(s).

Thus, while the ^1H NMR of AZM solution exposed for 6 h did not show any trace of either N-methylantranilic acid or anthranilic acid as an intermediate photoproduct, that exposed for 36 h clearly showed a significant amount of benzazimide as a final product. The role of benzazimide as a product was further investigated by irradiating a benzazimide methanol solution for 12 h; the ^1H NMR spectrum for benzazimide did not change, confirming that it is indeed photochemically stable to this UV-A irradiation, and thus a likely final product.

HPLC analysis was performed as another method of identifying the intermediate and products of the AZM photolysis. The chromatograms of unexposed AZM, anthranilic acid, N-methyl anthranilic acid, benzazimide and a mixture of all four compounds as water/methanol solutions were obtained to establish their retention times on the column used. The chromatogram of an AZM 60/40 water/methanol solution (which was found to give the best separation of the target compounds) photolyzed at 350 nm for 8 h showed two major peaks with retention times of 3.1 and 8.8 min; these matched perfectly to the retention times measured for BA and AZM standards, respectively. The concentration of BA after 8 h exposure was determined to be 7.0×10^{-5} M, which corresponds to 28% conversion of the initial 2.5×10^{-4} M, AZM, while the concentration of AZM remaining was determined to be 1.2×10^{-4} M, which corresponds to a 52% conversion overall. Thus, BA is clearly the major photoproduct, accounting for 54% of the photolyzed AZM. A much smaller peak than that identified as BA was also observed, with a retention time of 1.5 min. This value matched that of both NMA and AA standards, which were both found to elute with retention times of 1.5 min. Thus, we were only able to assign the intermediate as either NMA or AA, based on these HPLC measurements.

Thus, both HPLC and ^1H NMR show that benzazimide is the major stable photoproduct of AZM UV-A photolysis. No trace of anthranilic acid or N-methylantranilic acid could be observed by ^1H NMR, and a small peak which could only be assigned as either NMA or anthranilic acid was observed by HPLC. The lack of evidence for N-methylantranilic acid as an intermediate in the NMR studies, which was clearly observed by fluorescence, is a result of its very low concentration as an intermediate (the conversion at 8 h estimated to be approximately 4% using the fluorescence quantum yields, extinction coefficients and observed fluorescence enhancement), too low to be detected by NMR. The fact that it could clearly be detected by fluorescence is a result of its extremely high fluorescence quantum yield, which we measured to be 360 times larger than that of AZM. This tremendous fluorescence enhancement allows this intermediate to be detected by fluorescence at a

very low concentration, but not by NMR, for which there is no such signal enhancement.

3.3. Proposed mechanism for UV-A photolysis of AZM

Based on the experimental observation of N-methylantranilic acid as an intermediate (observed by fluorescence spectroscopy), and benzazimide as a final product (observed by ^1H NMR and HPLC), and taking into account mechanisms proposed in previous papers on AZM [6–10] and AZE [13], the mechanism shown in Scheme 1 is proposed for AZM UV-A photolysis.

The production of benzazimide as a primary photoproduct, as observed by both ^1H NMR and HPLC, agrees with the previous literature reports [7–9,11], and is proposed to occur via the pathway labeled Path 1 in Scheme 1, in agreement with the mechanism given in Ref. [9]. This pathway involves a homolytic cleavage of the C–N bond of the side chain to form a very short-lived radical pair, including a triazinone radical, which can form benzazimide via hydrogen atom abstraction. Whereas benzazimide has previously been proposed to undergo further photolysis to form anthranilic acid under UV-B irradiation [9], our studies show it to be photostable under UV-A irradiation. As discussed above, a separate photolysis experiment in which a solution of benzazimide was placed in the 350 nm photoreactor for 12 h confirmed its photostability at this wavelength.

N-methylantranilic acid was identified by fluorescence spectroscopy as the highly fluorescent, photochemically unstable intermediate photoproduct of AZM UV-A photolysis. This is proposed to occur via a second competing pathway to Path 1 described above for production of benzazimide as a stable product, and is labeled Path 2 in Scheme 1. Since N-methylantranilic acid is by far the most highly fluorescent compound involved in this photochemical scheme, the fluorescence-based kinetic experiments depicted in Fig. 2 and tabulated in Table 1 are in effect directly following Path 2, the formation and destruction of this intermediate, with k_1 corresponding to the growth of NMA and k_2 to its subsequent decay. This provides support for this proposed pathway, particularly based on the solvent and kinetic isotope effects observed for the decay step (k_2 in Table 1). This pathway is based on the mechanism proposed in reference 14 for AZE photolysis, and involves different cleavage of AZM, namely the homolytic cleavage of the C–S bond of the side chain, which results in the formation of a very short lived ketene upon removal of N_2 . Reaction of this ketene with water produces the highly fluorescent intermediate N-methylantranilic acid. This step is expected to be extremely fast, as ketenes are well known to react very rapidly with water [16]; there must have been sufficient water present in the methanol and deuterated methanol solutions for this to occur very rapidly even in these solvents.

Based on our photolysis results, N-methylantranilic acid then undergoes further photochemical decomposition. We propose that this photolysis of N-methylantranilic acid occurs via a photochemical decarboxylation from its excited state followed by hydrogen abstraction from the solvent to produce aniline, as shown in Scheme 1. This is in agreement with the observed deuterium isotope effect observed in methanol and discussed above, with this abstraction being the rate-determining step of the decay of N-methylantranilic acid. Aniline is stable to UV-A irradiation according to the literature [17], and was reported to be the final photostable product in the TiO_2 -catalyzed photolysis of AZM [11]. In addition, such photochemical decarboxylation involving loss of CO_2 is well known for aryl carboxylic acids [18,19]. Attempts to detect aniline in the product mixture were unsuccessful, presumably due to the very low overall quantum yield for its production. (It is also possible that photolysis of N-methylantranilic acid produces N-methylaniline instead of aniline, via cleavage of an N–H instead of the N– CH_3 bond prior to loss of CO_2 .)

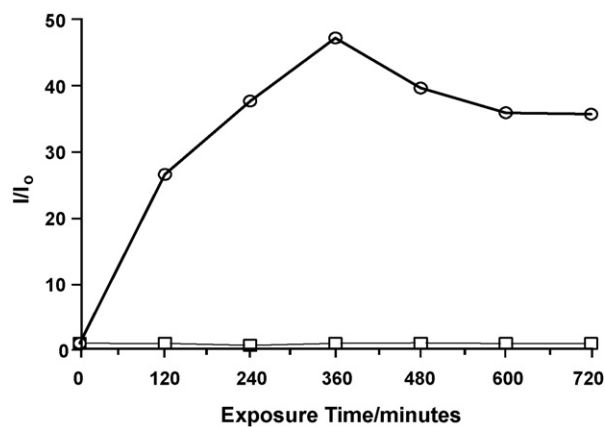


Fig. 5. The fluorescence of a 2.0×10^{-5} M solution of AZM in a natural water sample as a function of sunlight exposure time over the course of a single day (August 26, 2004) from 8:00 am to 8:00 pm (○), and that of an identical solution kept in the dark during the same period (□).

The overall mechanism proposed in Scheme 1 thus represents a combination of various mechanisms proposed previously in the literature (some of which were for other UV ranges), with new proposed steps to reflect our experimental observation of N-methylantranilic acid as the major observable intermediate, and benzazimide as a stable photoproduct, and presents a more complete mechanism for the photolysis of the important pesticide AZM under UV-A irradiation, such as that which occurs in the environment in shallow natural waters.

3.4. Photolysis of AZM by sunlight

Fig. 5 shows the fluorescence of a solution of AZM in water as a function of exposure to sunlight, compared to that of an identical solution kept in the dark. It should be noted that this was by necessity done at different times during the course of several sunny days in August (on the balcony of our chemistry building), and thus the intensity of the sunlight was not constant over the course of the total 12-h exposure. Therefore, these results cannot be analyzed to extract kinetic information, but are useful for qualitative determination of the effect of sunlight on AZM.

This figure clearly shows that sunlight can cause the same photolysis of AZM as that observed in the photoreactor. The shape of this plot is very similar to the shape of the plot shown in Fig. 2 for the photoreactor photolysis of AZM at 350 nm. This result has significant implications on the environmental fate of this harmful pesticide: in shallow, relatively clear streams, where sunlight can penetrate the water significantly, then sunlight must be considered as a major mechanism for removal of this pesticide. This is in addition to other degradation pathways, including reduction by aquatic macrophytes [20] and chemical oxidation [21]. In such natural waters under sunny conditions, the pesticide would be expected to be photolyzed over the course of a day or two.

4. Conclusions

Our results show that the UV-A photolysis of AZM results in the formation of N-methylantranilic acid as a primary photoproduct, which is in fact further photolyzed, most likely to aniline. This finding is different than that of previous studies of the UV-B photochemistry of AZM, which reported anthranilic acid as a photoproduct, but is in agreement with a previous study on the structurally similar pesticide azinphos-ethyl. Benzazimide was identified as the major photostable product, postulated to be produced in a parallel pathway involving a different initial cleavage

of AZM than that involved in production of N-methylantranilic acid. This again differs with previous studies using UV-B irradiation, under which benzazimide was found to be photolabile. These results emphasize the importance of irradiation wavelength in determining photochemical processes. The kinetics of this photolysis was conveniently measured using fluorescence spectroscopy, and fit to a three-species model with a first-order growth of a strongly fluorescent intermediate followed by its first order decay, in which N-methylantranilic acid is itself photolyzed, yielding aniline as the ultimate, stable photoproduct. This is the first fluorescence-based report on the photolysis of AZM, and has important implications for the UV-enhanced fluorescence-based trace analysis of this important pesticide, as over-exposure will reduce the fluorescence signal. Furthermore, the measurement of the kinetics provided information on the mechanism, in terms of polarity-dependence and deuterium isotope effects. It was shown that this photochemical degradation pathway also results from the absorption of sunlight; this has significant implications on the environmental fate of this pesticide. At least in shallow, relatively clear natural water systems, this sunlight-driven photolysis is expected to greatly reduce the residence time of AZM, probably to less than a day. A detailed mechanism for the UV-A photolysis of AZM has been developed, based on previous mechanisms reported in the literature for UV-B irradiation but also incorporating the new results obtained, providing a more complete and accurate description of the UV-A photochemistry of AZM, which also applies to the photolysis of AZM in natural waters by incident sunlight.

Acknowledgments

This work has been supported by the Natural Sciences and Engineering Research Council of Canada (NSERC). Acknowledgements

are made to Dr. Michael Liu, UPEI, for various photochemical discussions, and to Dr. Barry Linkletter, UPEI, for assistance with the HPLC experiments.

References

- [1] K.A. Hassall, *The Biochemistry and uses of Pesticides*, second ed., MacMillan, London, 1990.
- [2] A.G. Hornsby, R.D. Wauchope, A.E. Herner, *Pesticide Properties in the Environment*, Springer, New York, 1996.
- [3] D.K. Tanner, M.L. Knuth, *Ecotoxicol. Environ. Saf.* 32 (1995) 184–193.
- [4] R. Schulz, C. Hahn, E.R. Bennett, J.M. Dabrowski, G. Thiere, S.K.C. Peall, *Environ. Sci. Technol.* 37 (2003) 2139–2144.
- [5] Y. Yao, T. Harner, P. Blanchard, L. Tuduri, D. Waite, L. Poissant, C. Murphy, W. Belzer, F. Aulagnier, E. Sverko, *Environ. Sci. Technol.* 42 (2008) 5931–5937.
- [6] B.D. Wagner, A.C. Sherren, M.A. Rankin, *Can. J. Chem.* 80 (2001) 1210–1226.
- [7] D.G. Crosby, *Residue Rev.* 25 (1969) 1–12.
- [8] T.T. Liang, E.P. Lichtenstein, *J. Econ. Entomol.* 65 (1972) 315–321.
- [9] M. Ménager, X. Pan, P. Wong-Wah-Chung, M. Sarakha, *J. Photochem. Photobiol. A: Chem.* 192 (2007) 41–48.
- [10] M. Bavcon Kralj, M. Franko, P. Trebše, *Chemosphere* 67 (2007) 99–107.
- [11] P. Calza, C. Massolino, E. Pelizzetti, *J. Photochem. Photobiol. A: Chem.* 199 (2008) 42–49.
- [12] F. García Sánchez, A. Aguilar Gallardo, *Analyst* 117 (1992) 195–198.
- [13] J.L. Vilchez-Quero, J. Rohand, R. Avidad-Castañeda, A. Navalón, L.F. Capitán-Vallvey, *Frenius. J. Anal. Chem.* 350 (1994) 626–629.
- [14] W.M. Abdou, M.M. Sidky, H. Wamhoff, *Z. Naturforsch.* 42b (1987) 907–910.
- [15] D.F. Eaton, *J. Photochem. Photobiol. B: Biol.* 2 (1988) 523–531.
- [16] H.R. Seikaly, T.T. Tidwell, *Tetrahedron* 42 (1986) 2587–2613.
- [17] E.M. Sharshira, *Heterocycl. Commun.* 9 (2003) 527–534.
- [18] A.V. Willi, C.M. Won, P. Vilk, *J. Phys. Chem.* 72 (1968) 3142–3148.
- [19] W.L. Miller, M.A. Moran, *Limnol. Oceanogr.* 42 (1997) 1317–1324.
- [20] J.M. Dabrowski, E.R. Bennett, A. Bollen, R. Schulz, *Chemosphere* 62 (2006) 204–212.
- [21] K.M. Crowe, A.A. Bushway, R.J. Bushway, R.A. Hazen, *J. Agric. Food Chem.* 54 (2006) 9608–9613.